Detection of Icing and Related Loss of Control Effectiveness in Regional and Corporate Aircraft

William Ribbens*and Robert H. Miller†
Department of Aerospace Engineering,
University of Michigan,
Ann Arbor, MI 48109.

January 29, 1999

Abstract

This paper presents a method of detecting aircraft icing by monitoring its effects on aircraft dynamics. This paper shows that uncontrolled icing on control surfaces directly influences control effectiveness. Using data from onboard attitude and navigation sensors via highly computationally efficient algorithms, the control effectiveness is estimated, thereby detecting icing. Using actual flight test data from NASA Lewis Research Center, this paper demonstrates the ability of this method to detect the loss of elevator effectiveness that occurs with uncontrolled horizontal stabilizer icing that could result from a failed deicing boot. The method is generally applicable to loss of control effectiveness due to icing.

Icing affects the aerodynamic performance of aircraft by contaminating the aerodynamic surfaces. Without anti-icing equipment icing, if sufficiently severe, can relatively quickly lead to a situation in which controllable flight is impossible. Even aircraft with anti-icing equipment are potentially susceptible to icing under certain conditions. Some turboprop aircraft that have de-icing boots on the leading edge of aerodynamic surfaces may experience wing and tailplane icing behind the de-icing boots. Moreover, de-icing boots can fail due to a variety of conditions including holes produced by rocks etc. In particular the failure of a horizontal stabilizer boot can occur under such circumstances that the flight crew is unaware of the failure.

*SAE Fellow

†R.H. Miller is supported in part by NASA under grant NGT4-52404

1 Introduction

Ice accumulation on the horizontal stabilizer is a potentially hazardous condition particularly during approach and landing. Among other effects icing results in a major reduction of $C_{L_{max}}$ for any iced aerodynamic surface be it the horizontal stabilizer, vertical stabilizer, or main wing. During approach and especially during final approach phase of flight the flaps are deflected, causing an increase in downwash (relative to cruise for example) that can seriously reduce the tailplane stall margin.

It is the goal of the current study to detect icing by detecting the resulting changes in aircraft dynamics. The major focus for the present paper is to detect the loss of control surface effectiveness that results from icing via estimating changes in the aircraft dynamic model. In particular we consider the example of the loss of elevator effectiveness resulting from a failed de-icing boot during flight in icing conditions (as an illustration of the method).

The present method of ice detection has relevance to turboprop commuter or corporate aircraft that commonly use de-icing boots as the primary ice protection system. A significant number of these aircraft are in service both in part 135 as well as part 121 operations. However, it should be emphasized that the method of ice detection via loss of control effectiveness is potentially applicable to any controls

on any aircraft regardless of its ice protection system.

The concept here is to detect the loss of elevator effectiveness due to a failed de-icing boot at an early phase such that appropriate pilot action can be taken to safely complete the flight. In this method, the aircraft dynamics are continuously monitored by appropriate computer manipulation of data from the attitude and/or navigation sensors. Then once the loss of control effectiveness resulting from uncontrolled icing has been detected the flight crew can be notified through relevant display.

Other previous work Ref. [1] has attempted to detect icing via online parameter estimation however the present method is based upon continuously monitoring aircraft dynamics via a state estimator. This approach is highly computational efficient relative to online parameter estimation. This estimator is of the form of a gain scheduled Failure Detection Filter (FDF) as introduced in Ref. [2], which incorporates a state variable model for the aircraft dynamics in the aircraft body axes. The eigenstructure for the state estimator is chosen such that the output error residuals resulting from a hypothesized failure(eg. a failed de-icing boot on a horizontal stabilizer) are one dimensional. The hypothesized failure is readily detected by a statistically significant error residual and it can be isolated from other classes of failure by its direction in output space. Any other failure having a collinear output error residual, that is said to be detection equivalent to the hypothesized failure, produces the same change in aircraft dynamics as the hypothesized failure.

The FDF operates by estimating the aircraft instantaneous state vector $\hat{x}$ and computing the m estimated sensor outputs, $\hat{y}$, from $\hat{x}$. Then the residual error e between the actual, y where $y \in R^m$, and estimated sensor outputs, $\hat{y}$, is obtained:

$$e = y - \hat{y} \tag{1}$$

For a properly designed FDF, whenever there are no failures, the output error residual is very small (ideally zero). Whenever the hypothesized failure occurs, the error residual magnitude will be proportional to the failure and will be in the unique direction in output space that is associated with the given failure. Other failure or changes in aircraft dynamics have error residuals in different directions. A failure can be detected via the magnitude $\|e\|$ of the error residual. The failure can be isolated from other failures via the direction of the error residual in output space using straight forward decision logic.

A block diagram of the system is depicted in Figure 1.The inputs to the FDF include inputs to the aircraft and outputs of the attitude/navigation sensors. The FDF generates error residuals that are continuously monitored by the decision logic.

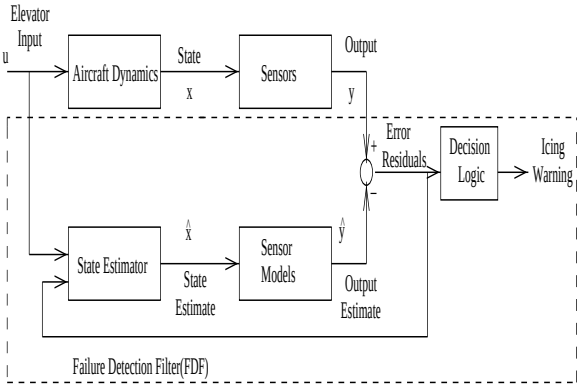

Figure 1: Failure Detection Filter Topology

2 Nonlinear Aircraft Model

The observer/state estimator applicable for the present method is derived from a state variable model for the aircraft dynamics. This state variable model is, in turn, derived from nonlinear models of the aircraft that are obtained from flight test data for the aircraft being modeled. These nonlinear models are constructed for the uniced aircraft as well as for that aircraft with artificial ice attachments (to the horizontal stabilizer) simulating actual icing. Nonlinear models are obtained for a variety of flight conditions including takeoff, landing and various cruise configurations. The method of obtaining the nonlinear models is explained in Ref. [3]. The data from which the models were obtained was generously provided by NASA Lewis Research Center (see also Refs. [4] and [5]).

Normally, the robustness of such a linear model is not a major issue for the FDF type observer since the closed loop error dynamics are designed to be at least asymptotically stable via the eigenstructure assignment. This stability is achieved during the design of the filter.

Considering the example of the failed horizontal stabilizer boot, the effect of icing that can occur on this surface include a gradual trim change as the ice accretes on the surface. In addition icing results in a dramatic change on the horizontal tail lift characteristics including a large reduction in $C_{L_{max}}$. This latter effect is manifest in the dynamic model as a change in the input matrix. This latter change is in the form of a failure event vector that is the input vector for the dynamics of the FDF. That is, this hypothesized failure results in an error residual along a unique direction in output space associated with horizontal stabilizer icing.

In this case, detection of horizontal stabilizer icing resulting for example from a failed de-icing boot can be achieved by monitoring the output error residuals along the direction associated with that hypothesized failure. Optimal signal detection methods are potentially applicable to reduce the 2 types of detection errors (i.e. false alarms and missed detections).

This paper develops the models associated with such a failure and explains the design of a relevant FDF. In addition the performance of the FDF is demonstrated in simulation and with actual data from NASA Lewis Icing Research Aircraft, [6] flying with simulated horizontal stabilizer ice.

The nonlinear models used in this paper were developed from flight test data of a NASA Lewis Twin Otter research aircraft. This aircraft was flown in a number of configurations for both uniced and simulated iced conditions. The iced condition corresponds to accumulated ice after 22 minutes flying with a failed horizontal stabilizer boot.

Various shapes were attached to the horizontal stabilizer of the twin otter to simulate different levels of tailplane icing. These simulated icing attachments were developed from actual ice accumulation in the NASA icing research wind tunnel.

Aircraft weight and balance were based on previous weight and balance information, [7], and computations to take into account the changes since the previous flight tests. In flight measurements of the fuel usage were used to compute the center of gravity and moments of inertia for post flight data processing.

The maneuvers were performed in a decoupled manner which allowed the longitudinal subset of the dynamics to be separated out. The control input was a classic elevator doublet. The power control was maintained at a nearly constant combined thrust coefficient of about $C_T = 0.1$, yielding a thrust of approximately $1000lbf$. Each maneuver lasted approximately 12 to 14 seconds.

There were two distinct flight test configurations analyzed: uniced and iced. For each case, flights were conducted with flap settings of $0°$, $10°$, $20°$, $30°$. The uniced configuration represents the nominal aircraft. The failed boot configuration represents the level of icing 22 minutes after a de-icing boot fails on an aircraft experiencing icing. The 22 minutes is derived from a FAA requirement.

The first step in the design of the FDF is to obtain the nonlinear models for the aircraft based upon the flight test data (see Refs. [4] and [5]). The structure of the nonlinear model is available from any standard text on aircraft control. The following equations, [8], were used to model the longitudinal dynamics of the twin otter icing research aircraft.

$$\begin{aligned} \dot{X} &= f(X,V) \\ \begin{bmatrix} \dot{u} \\ \dot{w} \\ \dot{\theta} \\ \dot{q} \end{bmatrix} &= \begin{bmatrix} -wq + \frac{F_x}{m} - g_x \\ uq + \frac{F_z}{m} + g_z \\ q \\ \bar{q}ScC_m/I_y \end{bmatrix} \end{aligned} \tag{2}$$

$$\begin{aligned} \bar{q} &= \frac{1}{2}\rho(u^2+w^2) & \alpha &= \tan^{-1}\left(\frac{w}{u}\right) \\ F_x &= \bar{q}SC_x + T_x, & F_z &= \bar{q}SC_z + T_z \\ g_x &= \sin(\theta)g, & g_z &= \cos(\theta)g. \end{aligned}$$

where C_x,C_z, and C_m are polynomials functions of α, q, and δ_e. A more detailed explanation of the variables and the model can be found in Ref. [9]. The functions used for the detection filter are of the form,

$$C_x = x_1\alpha + x_2\alpha^2 + x_3\delta_e + x_4 \tag{3}$$

$$C_z = z_1\alpha + z_2 q + z_3\alpha^2 + z_4\delta_e + z_5 \tag{4}$$

$$C_m = m_1\alpha + m_2 q + m_3\alpha^2 + m_4\delta_e + m_5. \tag{5}$$

The values for the different coefficients can be found in Ref. [9]. The outputs are

$$\begin{aligned} Y &= h(X) \\ Y &= \begin{bmatrix} \alpha \\ \theta \\ q \end{bmatrix} \end{aligned} \tag{6}$$

3 Linear Model for Failure Detection Filter Design

A linear approximate state space model can be derived from the nonlinear model in the form:

$$\dot{x} = Ax + Bu \quad (7)$$
$$y = Cx \quad (8)$$

where: $A \in R^{n\times n}$ is the state transition matrix, $B \in R^{p\times n}$ is the input matrix, $C \in R^{m\times n}$ is the observation matrix, p is the number of inputs, and m is the number of sensors.

The above linear model is valid for the uniced aircraft at any given flight condition. A model for an aircraft at the same operating condition but with ice accumulation has a similar structure. The continuous time matrices for the NASA Lewis Research aircraft can be obtained from the nonlinear model using a standard linearization algorithm such as LINMOD in MATLAB. An example set of A, B, and C matrices are given in the appendix.

It has been shown in Ref. [9] that the state transition matrix is essentially the same for both iced and uniced cases. However, the input for these two cases differs by an amount fd that is a function of the amount of ice present on the tail plane. The input under iced conditions $B_{iced}u$ is given by:

$$B_{iced}u = B_{nom}u + f_d \quad (9)$$

That is, the effect of tailplane icing on the aircraft dynamics can be treated as an additive input failure (f_d).

The major effect of f_d on the input is in the direction of the elevator input and, in a sense, f_d represents the change in elevator effectiveness. The major goal of this paper is to demonstrate that the onset of tail icing in an aircraft can be modeled as a partial actuator failure and that an FDF (Refs [2] and [3]) can be designed to detect this failure. Whenever the FDF produces a statistically significant error residual in the constrained failure direction one knows a failure has taken place.

The state estimator that is implemented in an FDF is of the form of a gain scheduled Luenberger observer which continuously computes an estimate of $\hat{x}$ of the state vector. Its dynamics are given by:

$$\dot{\hat{x}} = \bar{A}\hat{x} + \bar{B}u + D_g(y - \hat{y}) \quad (10)$$

where $\hat{y} = C\hat{x}$, and where $\bar{A}$ and $\bar{B}$ are the state transition and input matrices of the nominal reference model for the aircraft dynamics. In the present work, gain scheduling is via aircraft operating conditions. At the present time the optimal gain scheduling strategy is a subject of study. However, at a minimum, separate models are required for: takeoff, climb, cruise(several), descent, approach, and landing.

The state vector error dynamics are of the form

$$\dot{\epsilon} = (\bar{A} - D_g C)\epsilon + f_d \quad (11)$$

where $\epsilon = x - \hat{x}$ is the state error residual and f_d is the input "failure" due to icing. Normally there is sufficient design freedom(in choosing D_g) to permit the output error residuals($e = C\epsilon$) to be constrained to a one dimensional subspace. In addition, the eigenvalues can be placed as a compromise between rapid response and minimal random error due to process or measurement noise. Further research is being conducted in this area. In the above formulation the failure event vector f_d corresponds to the change in the input due to loss of control surface effectiveness.

4 Detection Space

Once the linear model for the aircraft has been obtained for a given operating condition the next step in the design of an FDF is to determine the detection space of the event vector. This is important as the detection space contains all the failure event vectors that are equivalent. Additionally the rank of the detection space indicates the number of poles of the estimator which are determined by the geometric constraints of the detection filter. Jones (Ref. [2]) defines the detection space of f_d, $\overline{\mathcal{R}}_1$, in the following manner.

Definition 1. Let f_d be an event vector associated with a failure in a system which is modeled in the un-failed state by (A, B, C). Let $Cf_d \neq 0$. The detection space for f_d is denoted by $\overline{\mathcal{R}}_1$ and is the direct sum:

$$\overline{\mathcal{R}}_1 = f_d \oplus \mathcal{R}_1 \quad (12)$$

where $\mathcal{R}_1$ is the largest subspace which satisfies the

three conditions:

$$\mathcal{N}(\mathcal{O}) \cap \mathcal{R}_1 = \emptyset \quad (13)$$

$$\mathcal{R}_1 \subset \mathcal{N}(C) \quad (14)$$

$$A\mathcal{R}_1 \subset \overline{\mathcal{R}_1} \quad (15)$$

where $\mathcal{O}$ is the system observability matrix.

The procedure to determine the detection space of f_d is straight forward and documented in Ref. [2]. Use the failure signature to define a decoupling feedback gain, D_f, and a new output matrix C_m,

$$D_f = Af_d((Cf_d)^T(Cf_d))^{-1}(Cf_d)^T \quad (16)$$

$$C_m = (I - Cf_d((Cf_d)^T Cf_d)^{-1}(Cf_d)^T)C \quad (17)$$

then form the system observability matrix, $\mathcal{O}$ for this system.

$$\mathcal{O} = \begin{bmatrix} C_m \\ C_m(A - D_f C) \\ \vdots \\ C_m(A - D_f C)^{n-1} \end{bmatrix}. \quad (18)$$

The detection space is then just the null space of this matrix, $\mathcal{O}$. Let $g = \overline{\mathcal{R}_1}$ and for a typical icing failure being investigated the detection space, g, is

$$g = \begin{bmatrix} -0.2457 \\ -0.9647 \\ 0.0005 \\ 0.0947 \end{bmatrix}, \quad (19)$$

and when passed through the output matrix C this results in the residual projection vector

$$g_c = Cg = \begin{bmatrix} -0.1716 \\ 0.0048 \\ 0.9852 \end{bmatrix}, \quad (20)$$

5 FDF Design Example

To illustrate the potential of the FDF for ice detection, we present a couple of examples flown by the NASA Twin Otter research aircraft. Both examples are derived from a flight condition that is representative of landing consisting of a trim airspeed of about 90 kt and a flap setting of 30°. The coefficients for the nonlinear model for this case can be found in Ref. [9]. The A and B matrices given in the appendix represent the linearized aircraft dynamic model at the above flight conditions for uniced and iced conditions.

In actual implementation, the FDF design was discretized to be comensurate with practical application in one of the aircraft on board computers (e.g. flight control computer).

6 FDF Design for Flight Test Data

The design of the FDF for the flight test data has four degrees of freedom. The closed loop poles must be selected. The first closed pole is the pole associated with the detection vector space. In this case the pole was placed at $\lambda = 0.97$. This roughly corresponds to the linearized short period dynamics, $w_{sp} = 3rad/sec$, sampled at 100Hz and was found to give good results. This choice for the first pole is a compromise between the tolerable dynamic errors made by the state estimator and its noise performance, although it is not an optimal choice. Further research needs to be done to determine the optimal choice for this pole location. The choice of this pole determines part of the total feedback gain, $D_g = D_{P1} + D_{P2}$, where

$$D_{P1} = (-\lambda f_d + Af_d)((Cf_d)^T(Cf_d))^{-1}(Cf_d)^T. \quad (21)$$

The system can then be decomposed into the unobservable part caused by this feedback gain and the still available observable part. The poles of the remaining observable part, (P =closed loop poles), were placed by using Linear Quadratic Estimator theory and for the example used above were placed at

$$P = \begin{bmatrix} 0.38 \\ 0.99 \\ 0.97 \end{bmatrix}. \quad (22)$$

7 Results

The performance of the FDF for detecting tailplane icing was evaluated both in simulation and with actual flight test data. The system of Figure 2 was constructed in a computer simulation environment using

SIMULINK/MATLAB. For the simulated system, the aircraft dynamics were represented by the nonlinear models obtained as explained in Ref. [9].

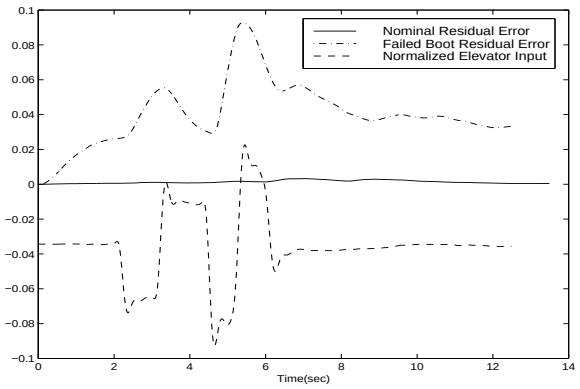

Figure 2: Simulated FDF Response

Figure 2 depicts the l_2 norm of the error residuals for the nominal and iced conditions. The elevator input doublet is also shown in this figure. Note that the error remains small even though the input excitation is relatively large. However, in the case of the iced elevator, the error residuals are significantly non zero throughout this test.

The relatively large error residuals of the above case indicate that a significant change in aircraft dynamics have occurred. However, the magnitude of the error (i.e., $\|e\|$) is not sufficient to indicate, by itself, that a loss of elevator effectiveness has occurred.

In order to identify that a loss of elevator effectiveness has occurred, it is necessary to also consider the direction of the output error residual. A second test of the FDF performance was conducted using actual flight test data for the aircraft dynamics. Once again, excitation is via an elevator doublet.

In order to isolate the change in aircraft dynamics and to demonstrate that it is the result of icing, the magnitude and direction of the error residuals are plotted. In this case, the angle between the error residual and the vector g_c representing the direction associated with icing induced loss of elevator effectiveness is shown. Figures 3 and 4 are plots of the magnitude off the error ($\|e\|^2$) and the angle between e and g_c($\angle e, g_c$). Figure 4 is the plot for the un-iced (nominal) aircraft and Figure 3 is the plot for the iced aircraft.

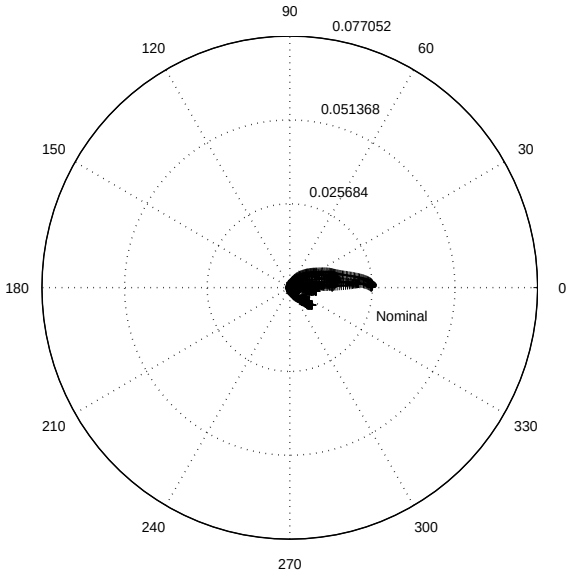

Figure 3: Nominal Un-Iced FDF Response

Ideally to perfectly identify that the change in dynamics is a result of icing (via elevator effectiveness), these two vectors should be collinear (i.e., the angle should remain 0. In practice however, owing to process and sensor noise, the error residual is actually a random process.

Nevertheless, note that the angle in Figure 4 remains small though non zero. The magnitude for the iced case is approximately 3 times larger than the maximum magnitude for the uniced case. Relatively straight forward decision logic can detect the iced from the uniced case.

8 Conclusions

Tests have also been conducted at other flight conditions with somewhat comparable results. Generally speaking, the error "signature" increased for increasing flap angles. We suspect that this result is due to the reduced stall margin for the tail for the higher flap angles. However, more flight testing of this method is desirable to conclude that the method is practically feasible. Nevertheless, the above results show potential for detecting ice via loss of elevator effectiveness.

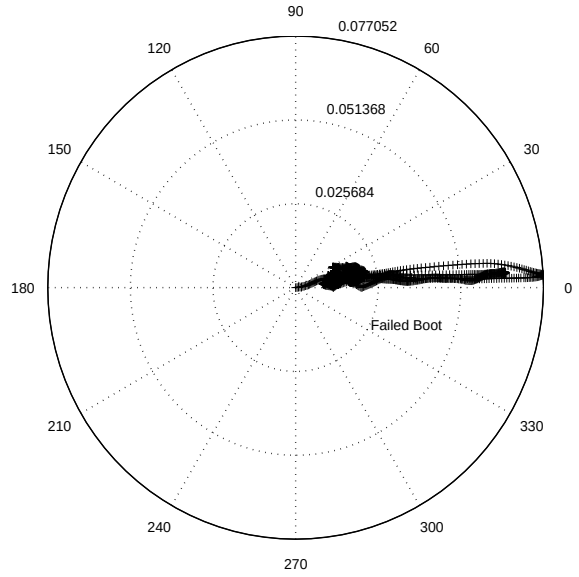

Figure 4: Failed Boot Iced FDF Response

References

[1] IFAC World Congress. *Parameter Identification for inflight Detection of Aircraft Iciing*, July 1999.

[2] Harold Jones. *Failure Detection in Linear Systems*. PhD thesis, MIT, 1973.

[3] Robert H. Miller and William B. Ribbens. Detection of the Loss of Elevator Effectiveness due to Icing. Number 99-0637 in 37th Aerospace Sciences. AIAA, Jan. 1999.

[4] Thomas P. Ratvasky and Judith Foss Van Zante. In-Flight Aerodynamic Measurements of an Iced Horizontal Tailplane. Number 99-0638 in 37th Aerospace Sciences. AIAA, Jan. 1999.

[5] Judith Foss Van Zante and Thomas P. Ratvasky. Investigation of Dynamic Flight Maneuvers with an Iced Tailplane. Number 99-0371 in 37th Aerospace Sciences. AIAA, Jan. 1999.

[6] Thomas P. Ratvasky and Judith Foss Van Zante. NASA/FAA Tailplane Icing Program Overview. Number 99-370 in 37th Aerospace Sciences. AIAA, Jan. 1999.

[7] T.P. Ratvasky and R.J. Ranaudo. Icing Effects on the Aircraft Stability and Control Determined from Flight Data. Technical Report 105977, NASA, 1993.

[8] John H. Blakelock. *Automatic Control of Aircraft and Missles*. John Wiley, 2nd edition edition, 1991.

[9] Robert H. Miller and William B. Ribbens. The Effects of Icing on the Longitudinal Dynamics of an Icing Research Aircraft. Number 99-0636 in 37th Aerospace Sciences. AIAA, Jan. 1999.

9 Appendix

An exmaple of the nominal and iced A, B, and C matrices for the operating point Y_{eq} and X_{eq} are given below.

$$Y_{eq} = \begin{bmatrix} 0.0625 \\ 0.0369 \\ 0 \end{bmatrix}$$

$$X_{eq} = \begin{bmatrix} 59.43 \\ 3.72 \\ 0.0369 \\ 0 \end{bmatrix}$$

$$A_{nom} = \begin{bmatrix} -0.0309 & 0.1706 & -9.8033 & -3.7222 \\ -0.2372 & -1.5028 & -0.3623 & 58.0423 \\ 0 & 0 & 0 & 1.0000 \\ 0.0058 & -0.0928 & 0 & -2.5489 \end{bmatrix}$$

$$B_{nom} = \begin{bmatrix} 1.3066 \\ -3.1814 \\ 0 \\ -7.7234 \end{bmatrix}$$

$$C_{nom} = \begin{bmatrix} -0.0010 & 0.0168 & 0 & 0 \\ 0 & 0 & 1.0000 & 0 \\ 0 & 0 & 0 & 1.0000 \end{bmatrix}$$

$$A_{iced} = \begin{bmatrix} -0.0316 & 0.2176 & -9.8033 & -3.7222 \\ -0.2447 & -1.5451 & -0.3623 & 56.2042 \\ 0 & 0 & 0 & 1.0000 \\ 0.0040 & -0.0875 & 0 & -2.8063 \end{bmatrix}$$

$$B_{iced} = \begin{bmatrix} 0.9272 \\ -4.8143 \\ 0 \\ -7.5778 \end{bmatrix}$$

$$C_{iced} = \begin{bmatrix} -0.0010 & 0.0168 & 0 & 0 \\ 0 & 0 & 1.0000 & 0 \\ 0 & 0 & 0 & 1.0000 \end{bmatrix}$$

Although the A_{nom} and A_{iced} appear different the eigenvalues have changed only slightly. The eigenvalues are

$$Eig(A_{nom}) = \begin{bmatrix} -2.0231 + 2.2652i \\ -2.0231 - 2.2652i \\ -0.0182 + 0.1796i \\ -0.0182 - 0.1796i \end{bmatrix},$$

$$Eig(A_{iced}) = \begin{bmatrix} -2.1712 + 2.1307i \\ -2.1712 - 2.1307i \\ -0.0203 + 0.1695i \\ -0.0203 - 0.1695i \end{bmatrix}.$$

The failure event vector, f_d, is

$$F_d = \begin{bmatrix} 0.3794 \\ 1.6329 \\ 0 \\ -0.1456 \end{bmatrix}.$$